

# Tele-Operated High Speed Anthropomorphic Dextrous Hands with Object Shape and Texture Identification

P.Y Chua

[chuapingyong@yahoo.co.uk](mailto:chuapingyong@yahoo.co.uk)

D.G. Caldwell

[d.g.caldwell@salford.ac.uk](mailto:d.g.caldwell@salford.ac.uk)

M. Bezdicek

[m.bezdicek@pgr.salford.ac.uk](mailto:m.bezdicek@pgr.salford.ac.uk)

S. Davis

[s.davis@salford.ac.uk](mailto:s.davis@salford.ac.uk)

Advanced Robotics, School of Computing, Science and Engineering

The University of Salford

Salford, Greater Manchester, U.K.

**Abstract - This paper reports on the development of two Tele-Operated High Speed Anthropomorphic Dextrous robotic hands. The aim of developing these hands was to achieve a system that seamlessly interfaced between humans and robots.**

To provide sensory feedback to a remote operator tactile sensors were developed to be mounted on the robotic hands. Two systems were developed, the first, being a skin sensor capable of shape reconstruction placed on the palm of the hand to feed back the shape of objects grasped and the second is a highly sensitive tactile array for surface texture identification.

**Index Terms – Robotic Hands, Pneumatic Muscle Actuator, Skin Sensor, Tactile Array, Shape/Texture Identification .**

## I. INTRODUCTION

The human hand other than the feet is the most applied part of the human body in our daily endeavour. As a result we become expert at controlling it and are able to perform the most delicate of manipulation tasks. When the hand is neither strong enough nor tough enough to handle an object directly, its dexterity allows us to create tools to achieve the goal. Aristotle the great philosopher argued that man can defend himself far better than any other animal because of the unique construction of the human hand he wrote:

*“...But to man numerous modes of defence are open, and these, moreover, he may change at will; as also he may adopt such weapon as he pleases, and at such times as suit him....the fingers are well constructed for prehension and for pressure. One of these also, and this not long like the rest but short and thick, is placed laterally. For were it not so placed all prehension would be as impossible, as were there no hand at all. For the pressure of this digit is applied from below upwards, while the rest act from above downwards; an arrangement which is essential, if the grasp is to be firm and hold like a tight clamp.”*- Aristotle, Parts of Animals [1]

As observed by Aristotle prehension (grasping) is the essential function of the hand. This is largely due to the position and structure of the thumb. The lack of specialisation in the hand provides adaptability and creativity. With this it functions both as an output

(manipulation of objects) and input (sensitive and accurate sensory receptor) organ.

The human hand therefore is without doubt the perfect model in the development of a mechanical hand, hence the development of anthropomorphic dextrous hands that closely resemble it. A number of robotic hands have been developed which focus on either anthropomorphic design or dextrous design, often sacrificing one for the other due to the obvious complexity of developing a hand that closely emulates the human hand. Some anthropomorphic designs includes the Utah/MIT hand [2], Anthrobot Hand [3], Robonaut Hand [4, 5], DLR-Hand I & II [6, 7] and Ultralight hand [8]. Examples of hands whose main focus is on dexterity are the Salisbury hand [9], the Karlsruhe hand [10], the hand developed at the Technical University of Darmstadt [11], [12] and the Delft University hand [13].

Humans are blessed with the ability to manipulate their hands with great expertise and to perform a vast range of tasks using them. For this reason robotic hands can be of significant value in telepresence applications. To enable remote operation of a robotic hand an interface must be designed to reflect the movements of the operator's hand to the robot. The speed at which the mechanical hand can respond is crucial as a large delay in the reflection of the movement of the operator's hand would result in constrained movement and not a true reflection of the capability of the human hand.

This work seeks to develop a robotic hand which can be combined with a high fidelity data glove interface to allow teleoperation tasks to be performed. The specific aim is to produce a hand with the following features:

1. Anthropomorphism – having similar shape and size to the average human hand
2. Dexterity - Ultimately to have the same degrees of freedom as the human hand with equivalent dexterity
3. Speed - Ensuring no or little delay between the robotic hand and operator's hand movements.
4. Tactile feedback - Tactile sensors for feedback of environmental features which can aid remote operators.

Section II of this paper describes the mechanical design of a 19 DOF hand. This is followed by descriptions of both the actuation and control hardware used to operate the hand.

Section V describes tests performed using the hand, the results of which led to the development of a second hand with greater dexterity than the first. The final part of the paper describes two tactile sensors developed to be fitted to the hands which feedback data on the shape and texture of objects being handled to a remote operator.

## II. 19 DEGREES OF FREEDOM (DOF) MECHANICAL HAND

A robotic hand consisting of 19 DOF was designed and constructed consisting of four fingers, a thumb and a solid palm. Table\_1 shows the range of motion for each of the finger joints. The hand was formed from polyethylene due to its good frictional characteristics with the joints being constructed using steel pins.

Power from the actuators is transmitted to the fingers via braided nylon tendons with a tensile strength of 1250N as can be seen in figure 1. Extension and abduction of the fingers and thumb is achieved using return springs located in the palm and back of each finger. Routing of the tendons is achieved using additional steel pins.

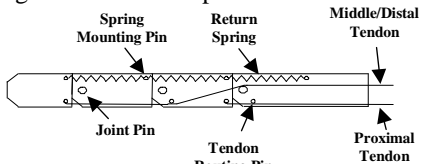


Figure 1 Tendon routing through the finger

The distal joints of all four fingers are coupled to the middle joint as can be seen leading to 15 active DOF, each is activated (flexion and adduction) by a single actuator located in the robot's forearm.

	1st	Middle	Ring	Little
Base	-5° → 40°		-5° → 30°	-5° → 40°
Proximal	0° → 90°	0° → 90°	0° → 90°	0° → 90°
Middle	0° → 110°	0° → 110°	0° → 110°	0° → 110°
Distal	0° → 90°	0° → 90°	0° → 90°	0° → 90°

Table 1 – Range of joint angle for robot hand.

## III. ACTUATION

Selection of an appropriate actuation system is critical to the success of the hand. The actuator must be capable of delivering forces with high fidelity for fine manipulation and at levels adequate for power grips. It also needed to have dynamic performance that could provide a fast response to operator inputs. An actuator providing a degree of compliance would also be desirable as it would allow the hand to experience shock impacts without becoming damaged.

The actuator chosen is the Pneumatic Muscle Actuators (pMA) derived from the McKibben muscle [16]. The pMA was chosen because it offers the following features:

1. Similar operation to the human muscle, it contracts in length when inflated and relaxes when deflated.
2. Muscles can be produced to any desired length or size with larger diameter muscles producing higher forces. This allows actuators with similar power to humans to be selected.
3. Exceptionally high power/weight and force/area ratio. Peak forces per cross sectional area greater than 500N/cm<sup>2</sup> (at 500KPa) have been achieved [16] and the muscles used weigh approximately 50g.
4. Safe operation due to inherent compliance with air being the only by product.
5. Muscles can be constructed quickly with minimal skill and replaced easily.
6. The pMA can achieve accuracy better than 1% for both displacement and force with a system bandwidth of up to 5Hz.
7. Since the pMA is flexible it is tolerant to rotational and lateral misalignment.

The pMAs used in this work have a maximum length of 280mm, a minimum diameter of 12mm and can generate a maximum force, at 3bar operating pressure, of 460N. The actuators were located in the robot's forearm with forces being transmitted to the hand via tendons as can be seen in figure 2.

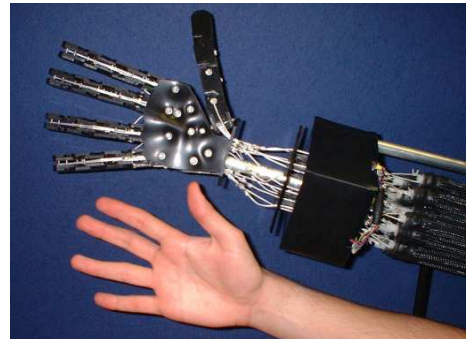


Figure 2 The 19 DOF Hand

## IV. CONTROL HARDWARE

Pneumatic valves are required to control the flow of air to the actuators. The valves used (MATRIX) have an airflow rate of 100NL/min at 6 bar drive pressure and they are driven by a 100Hz PWM signal generated by an Atmega8 microcontroller.

To enable closed loop control of the joint positions the hand uses linear potentiometers to determine joint angles. The sensors measure the motion of individual tendons and from this information joint angles can be calculated. The sensors are located remotely from the joints in an enclosure at the robots wrist. This ensures there is no movement of electrical connections to the sensors as the fingers move so reducing the likelihood of failure.

Joint angle data is fed to the ADC on the microcontroller where it is used in a control loop to modify the PWM signal to the valves and adjust the pressure in the muscles. A control board consisting of 2 microcontrollers with supporting circuitry was developed and attached to a block of 8 valves (4 for filling and 4 for venting) this provided control for 4 muscles. Four sets of valves and control boards were then daisy chained together and through a bus connected to a hub board consisting of an Atmega128 microcontroller, Bluetooth chip and supporting circuitry. The Bluetooth chip provides a communication link with a data glove which provides the necessary input signals for the manipulation of the mechanical hand.

The finger phalanges in the robotic hand are simple levers which convert tendon movement into joint motion. This however, presents a control problem as the effective lever length varies as the joint bends resulting in the rapid increase of torque applied to the joint as the finger flexes from full extension. This problem was overcome by implementing a triple integral in the PID control system resulting in the PI<sup>3</sup>D control system. The cube of the integral ensures that the system control output signal increases rapidly with positive control input and reduce rapidly with negative control input overcoming the problem described. However the down side is that the system becomes less stable. There are several methods to overcome this and still give a controller that does the job best [17, 18, 19]. A delay,  $\sigma$ , was added before the control loop as there is a time delay in the switching of the control valves. The tuning of this delay is important as too short a delay would result in the integral reaching its maximum limit before switching occurs while too long a delay results in over contraction of the muscle. Both situations result in an uncontrollable system.

The control system was further improved in the second hand designed (24 DOF mechanical hand) by adding pressure sensors to the control board for each muscle effectively adding an extra control loop. This also allows the maximum force that each muscle can deliver to be adjusted by limiting the maximum working pressure of each muscle and also allows a higher drive pressure than the actual working pressure of the muscles to be used, increasing the air flow through the valves and increasing the response time of the hand. The electronics of the control board was also modified to allow the switching of the PWM to be increased to 200Hz. With these modifications a finger flexion speed faster than that of the human hand can be achieved.

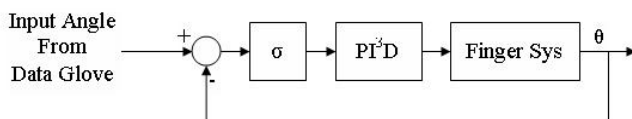


Figure 2 simplified Control Block Diagram for a Single Joint

## V. EXPERIMENTAL RESULTS

To assess the performance of the hand extensive testing was performed. Firstly to test the reliability of the hand a test rig consisting of a single finger was produced. This enabled the finger to be repeatedly cycled to identify points of likely failure. The test finger operated more than 100,000 times without failing.

To test the dexterity and speed of the robotic hand, a data glove was used. The data glove is available from CyberGlove® and was used with a specially designed Bluetooth circuit to interface with the hand. The dexterity of the hand was tested by grasping objects of different shapes and sizes. Fig. 3 shows the hand being used to manipulate a range of objects. The opposable thumb is evident in the grasping of the screwdriver where a centralised grip is achieved without the need of a wrist.

Finally the control system discussed in the previous section was tested to determine the speed of hand operation. Fig. 4 shows the total time taken for hand closure from fully open to be 0.72 sec. The speed of the hand was further demonstrated by catching a ball as shown in Fig. 5

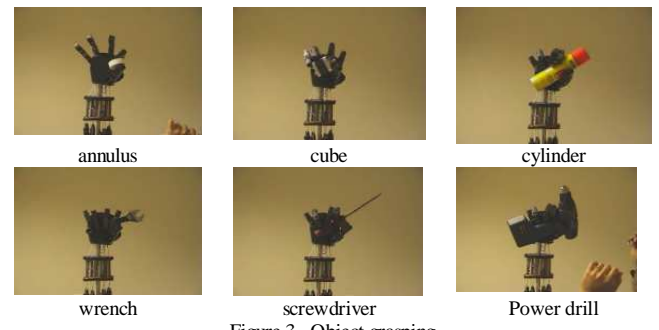


Figure 3 Object grasping

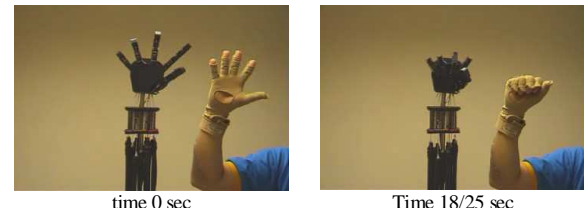


Figure 4 Total time from fully open to close is 0.72 sec

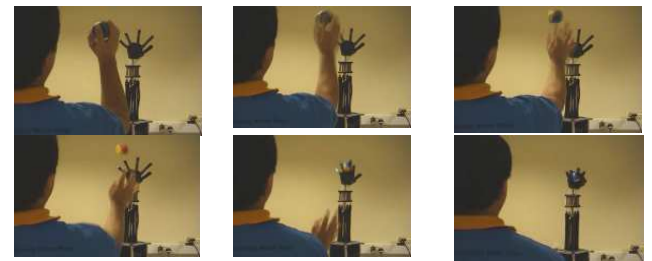


Figure 5 Ball catching sequence

## VI. 24 DEGREES OF FREEDOM (DOF) MECHANICAL HAND

After the successful testing of the 19 DOF hand a new 24 DOF hand was developed based on it. The aim being to develop a hand with even greater dexterity and a more anthropomorphic design.

To further increase the dexterity of the hand a flexible palm was added (Figure 7). The flexibility in the palm allows it to curl around a cylindrical/round object resulting in improved grasp stability. This also allows a more central grip to be achieved when grasping objects such as a screwdriver, or fork, etc. To further increase the range of tasks the hand could achieve a 2 DOF wrist was also added.

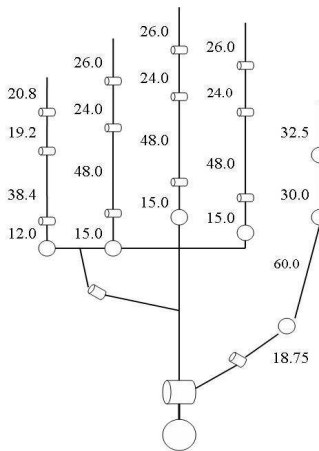


Figure 6 Kinematic chain of the 24 DOF hand



Back of hand



The palm side of hand

Figure 7 The 24 DOF Mechanical Hand



Hand complete with muscles

The addition of the wrist and flexible palm increases the anthropomorphism of the hand as it more closely resembles

the human hand than the 19 DOF hand. The proportions and sizes of the phalanges in each digit of the 24 DOF hand were based on the dimensions of an average human male hand. The distal phalanx of each of the fingers and the thumb have rounded ends with flattened pulps to further improve anthropomorphism.

The completed hand (Figure 7) was constructed from Aluminium with sensors located at each joint (direct sensing), reducing errors and allowing more accurate manipulation of small objects.

In telepresence/teleoperation applications tactile feedback from an object being handled can greatly improve the operators ability to manipulate objects. For this reason tactile sensors were developed which could be fitted to the hand and which would provide a remote operator with information about the shape and texture of objects being grasped/touched.

## VII. SKIN SENSOR FOR OBJECT SHAPE IDENTIFICATION

A skin sensor was developed, for location on the palm of the robot hand, which aimed to maximize the sensing area while keeping the number of sensors to a minimum. A prototype skin was developed having 16 tactels formed from 2 layers of 4 isolines of strain gauges etched from flexible PCB laminate with a copper thickness of 0.035mm and a flexible film thickness of 0.05mm. Each gauge has ten tracks of 0.25mm thickness, a total width of 5.4mm, a length of 60.5mm, a resistance of 0.7 Ω and a gauge factor of 4.5. The gauges are embedded in latex for protection and to unify their deformation

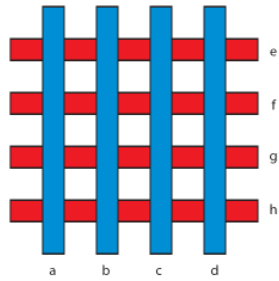


Figure 8 Skin sensor geometry configuration of the gauges

When an object is placed on the skin, information about its shape can be determined from the bending radius of corresponding strain gauges. This can be achieved using two different approaches. Firstly, by multiplying orthogonal gauges resulting in,

$$\begin{pmatrix} a \\ b \\ c \\ d \end{pmatrix} \times (e \quad f \quad g \quad h) = \begin{pmatrix} a \cdot e & a \cdot f & a \cdot g & a \cdot h \\ b \cdot e & b \cdot f & b \cdot g & b \cdot h \\ c \cdot e & c \cdot f & c \cdot g & c \cdot h \\ d \cdot e & d \cdot f & d \cdot g & d \cdot h \end{pmatrix}$$

Where the first vector shows readings from the horizontal gauges and the second vector from the vertical gauges and the 4x4 matrix gives the pressure at the strain gauge crossover points. This approach is more suitable when the deformation is more concentrated. The second method uses the sum of the deformations of the orthogonal gauges resulting in,

$$\begin{pmatrix} a & a & a & a \\ b & b & b & b \\ c & c & c & c \\ d & d & d & d \end{pmatrix} \begin{pmatrix} e & f & g & h \\ e & f & g & h \\ e & f & g & h \\ e & f & g & h \end{pmatrix} = \begin{pmatrix} a+e & a+f & a+g & a+h \\ b+e & b+f & b+g & b+h \\ c+e & c+f & c+g & c+h \\ d+e & d+f & d+g & d+h \end{pmatrix}$$

This approach is suitable when the deformation is not concentrated but spread over a wider area.

By adding a soft material (e.g. foam) on one side of the skin, pressure and force exerted by an object on the opposite side can be measured. If the material properties of the soft material are known the value of the force and pressure applied can be computed. Figure 9 shows impressions of different objects on the skin.

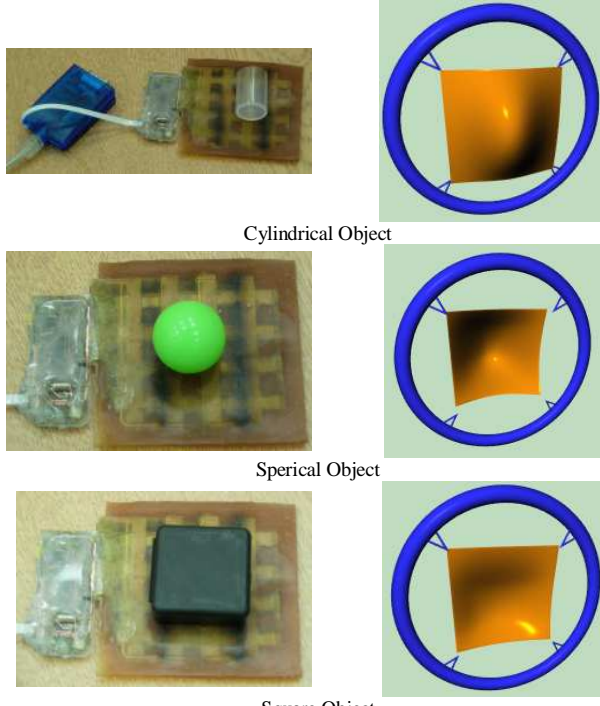


Figure 9 Impressions of different objects on skin

### VIII. TACTILE SENSOR ARRAY FOR TEXTURE IDENTIFICATION

The second sensor developed took the form of a sensor array. This consisted of three main parts, active sensing nodes located at the fingertips, mechanical coupling to transmit the signals from the potentially high impact surface of the skin to a safer sensor location and precision optical reflective sensors to convert the sensory data into high resolution tactile data.

The active sensing node is made up of a modified spring probes [14] designed for sensitivity and robustness. The probes, whose dimensions are shown in Figure 10, are formed in three section:

- i). Plunger (Beryllium copper, rhodium plated) giving good robustness, strength and tip resolution,
- ii). Barrel (Phosphor bronze, gold plated) providing strength, low friction, good robustness and sensitivity
- iii). Spring (music wire, gold plated)

The spring was removed to permit remote coupling to the optic sensor. Five of these probes were attached together in a row at 1mm tip to tip separation (Figure 11) to form an array.

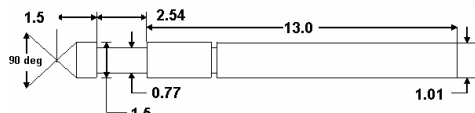


Figure 10 Two Part Spring Probes



Figure 11 Sensor Line Array

To enable the sensors to be mounted at the finger tips of a robot hand the reflective sensors needed to be remotely located due to limited space. The probes were therefore, mechanically coupled to the reflective surfaces via flexible plastic covered steel wires (0.67mm in dia.) which moved through PTFE sleeving with a bore diameter of 0.89mm and a wall thickness of 0.30mm. The reflective surface is made of polished Aluminum cylinders and allows for the optical coupling to the optical sensors. The close tolerance between the coupling wire and the sleeving ensure accurate displacement transmission while the materials selected ensure low friction (<0.05N). A cylinder made of black nylon completes the opto-coupler. The cylinder screens out ambient light to block out any interference from external infra-red light and ensures that the sensor only detects reflected infrared from the sensor tip reflector. It also serves as the housing for a spring that ensures the pin returns to its extended position when no force is applied and a smooth sliding sleeve for the reflector.

The optical sensor is a 655nm precision optical reflective sensor from Agilent Technologies [15]. This sensor is normally employed in bar code scanners with a lateral resolution 0.178mm. However, when this sensor is used in conjunction with a reflector (Figure 12) the resolution of the detected reflector movement normal to the sensing area can be as high as 1μm, dependent on the amplifier used, the reflective surface and the filtering of ambient light. For this

reason this system is well suited to the sensitivity needs of this project.

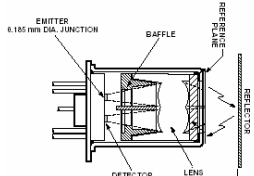


Figure 12 Optical Sensor with Reflector

The detailed surface profiles of three different materials were tested and presented. Each of these materials was chosen based on the human sensitivity of touch.

First, a 15cm metal ruler was chosen as it provides not only a regular pattern for comparison but we can also visually confirm the tactile profile. Figure 13 shows the profile of the steel ruler determined using the sensor array. Different colour in the plot represents different measured depths. The plot clearly shows great detail of the profile as graduations on the ruler are clearly evident as are the engravings.

Next the tactile pattern of wood was tested, this can be considerably different from what is observed visually as it is the woods grain that is observed not the tactile profile. The wood chosen had a tactile profile that was barely detectable to humans with a static touch but which becomes more clear when the surface is stroked with the finger. In other words the tactile profile is only clearly evident through vibrotactile (dynamic) sensing. Tests on wood would therefore provide clear evidence of the vibrotactile capability of the sensor array

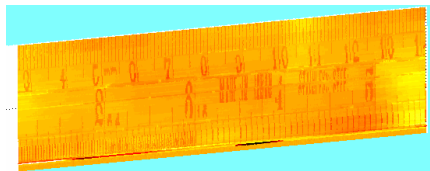


Figure 13 Surface Profile of the 15cm steel ruler reconstructed from tactile data

Figure 14 shows the data from two different sets of sensor readings taken at 100 $\mu$ m separation. The deepest valley shown in the 2 graphs represent a valley found on the test material. In the top figure, the depth of the valley is less compared with that observed in the second figure. This is due to the fact that generally valleys found on wood are limited in length across the surface of the wood. As we near the end of the valley the depth tends to reduce. Subsequent neighboring readings showed the depth reducing further and finally the valley disappearing. From the 2 graphs we can also observe the coincidence of each peak and valley.

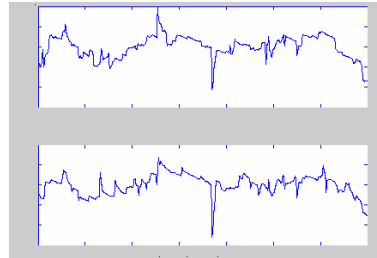


Figure 14 Reading taken from neighboring sensors

The final material chosen for testing was a fine surface plastic. The plastic surface feels completely smooth to the human touch when stroked with the finger. However when the surface is stroked with the fingernail the tactile characteristic becomes clear. Figure 15 shows the surface profile of the plastic sheet used as the test material

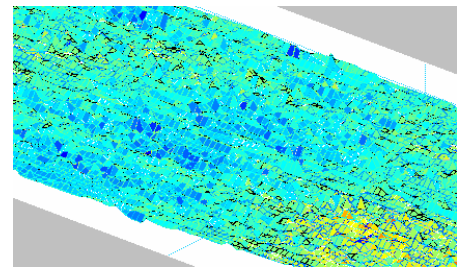


Figure 15 Surface profile of plastic

## IX. CONCLUSION

This paper has described the development of two robotic hands which have been shown to have both good anthropomorphism and dexterity. The hands are similar to the human hand in terms of size, shape and joint motions. The dexterity of the hands has been demonstrated through the grasping of different objects and its speed of motion has been assessed through a series of ball catching experiments. The hand has been used in conjunction with a data glove which has allowed teleoperation.

To further enhance the hands suitability to teleoperation tasks two tactile sensors have been developed to feed back information to a human operator. A skin sensor to be placed on the palm of the hand can clearly determine the shape of different objects pressed against it and a sensor array has been shown to detect both static and dynamic characteristics that allow it to clearly identify fine features of different materials.

Future work will combine the robotic hand and tactile sensors into a single platform and testing will be performed to identify the shape and texture of objects grasped.

## REFERENCES

- [1] Aristotle. "On the Parts of Animals, Book IV. Part 10. Translated by William Ogle. The Internet Classics Archive by Daniel C. Stevenson, Web Atomics", World Wide Web presentation is copyright © 1994-2000, Daniel C. Stevenson, Web Atomics

- [2] Jacobsen, S.C., Wood, J.E., Knutti, D.F., Biggers, K.B. “*The Utah-MIT dexterous hand: work in progress*”, The int. journal of robotics research, vol. 3, no. 4, pp. 21-50. 1984
- [3] Ali, M.S., Kyriakopoulos, K.J. Stephanou, H.E. “*The kinematics of the Anthrobot-2 dexterous hand*”, Proc. IEEE int. conf. on robotics and automation pp. 3\_705-3\_710. 1993
- [4] Lovchik, C. S., Diftler, M. A. “*The robonaut hand: A dexterous robot hand for space*”, Proc. Of the 1999 IEEE int. conf. on robotics and automation, pp. 907-912. 1999
- [5] Engelberger, G. “*NASA’s robonaut*”, Industrial robot: and international journal, vol. 28, no. 1, pp. 35-39. 2001
- [6] Butterfass, J., Hirzinger, G., Knoch, S. Liu, H. “*DLR’s multisensory articulated hand. Part I: Hard- and software architecture*”, Proc. of the 1998 IEEE int. conf. on robotics and automation, pp. 2081-2086. 1998
- [7] Butterfass, M., Gebenstein, H. Liu, H., Hirzinger, G. “*DLR-Hand II: Next generation of a dexterous robot hand*”, Proc. IEEE int. conf. on robotics and automation. 2001
- [8] Schulz, S., Pylatiuk, C., Brethauer, G. “*A new ultralight anthropomorphic hand*”, Proc. of the 2001 IEEE int. conf. on robotics and automation. 2001
- [9] Salisbury, J.K., Brock, D.L., Chiu, S.L. “*Integrated language, sensing and control for a robot hand*”, Proc. 3<sup>rd</sup> ISRR, Gouvieux, France, MIT press, Cambridge MA. 1985
- [10] Wöhlke, G. “*A programming and simulation environment for the Karlsruhe dexterous hand*”, Journal of robotics and autonomous systems, vol. 9, pp. 243-263. 1990
- [11] Paetsch, W., Kaneko, M. “*A three finger multijointed gripper for experimental use*”, Proc. IEEE int. works on intelligent robots and systems, IROS’90. 1990
- [12] Weigl, A., Seitz, M. “*Vision assisted disassembly using a dexterous hand-arm system: an example and experimental results*”, Proc. IFAC int. symp. On robot control, SYROCO,94, pp. 314-322. 1994
- [13] Jongkind, W. “*Dexterous gripping in a hazardous environment*”, Ph.D. Thesis, Delft Univ. of Technology. 1993
- [14] Harwin Plc, Fitzherbert Road, Farlington, Portsmouth, Hants, PO6 1RT, United Kingdom.
- [15] Agilent Technologies UK Ltd., South Queensferry, West Lothian. EH30 9TG, United Kingdom.
- [16] Davis, S. T. “*Braided pneumatic muscle actuators. Enhanced modeling and performance in integrated, redundant and self healing actuators*”, Ph.D. Thesis, The University of Salford, U.K. 2005
- [17] Niculescu, S. I., Michiels, W. “*Stabilizing a chain of Integrator using multiple delays*”, IEEE trans. On automatic control, vol. 49, no. 5. 2004
- [18] N. Marchand ,A. Hably, “*Nonlinear stabilization of multiple integrators with bounded controls*”, Automatica, vol. 41, no. 12, pp 2147-2152, 2005
- [19] M. Balas “*Tracking Inaccessible Signals in Linear Systems*” AIAA Guidance, Navigation, and Control Conference and Exhibit, Providence, Rhode Island, Aug. 16-19, 2004